Numerical Calculations with a Multi-layer Model of Mixed Sand Transport Against Measurements in Wave Motion and Steady Flow

Leszek M. Kaczmarek
Koszalin University of Technology, Poland
https://orcid.org/0000-0003-4557-2195

Iwona Radosz[*]
Koszalin University of Technology, Poland
https://orcid.org/0000-0002-1539-2364

Jerzy Zawisza
Koszalin University of Technology, Poland
https://orcid.org/0000-0002-4076-4115

[*]corresponding author's e-mail: iwona.radosz@tu.koszalin.pl

Abstract: A multi-layer model is used to calculate time-dependent sediment velocity and concentration vertical profiles. This model, in which the differences in sediment transport at different distances from the bed are considered is intended both for the wave motion and steady flow. Numerical calculations were carried out for sediment transport during the wave crest and trough and total sediment transport as a sum of their absolute values. The model concept of variation in shear stress from the skin stress value above the bed to the stress value at the bed previously proposed for steady flow is extended here for the wave motion and verified by direct stress measurements. The calculations were carried out for mixed sand sediments with different grain size distributions including semi-uniform and poorly sorted grains. Comparison with the available small- and large-scale data from flumes and oscillating tunnels yields agreement typically within plus/minus a factor two of measurements.

Keywords: wave motion, steady flow, sediment transport, transport during the wave crest and trough

1. Introduction

There are several works representing a multi-phase approach to sediment transport modelling. Berzi and Fraccarollo (2016) present an interesting description of multilayer sediment transport for steady flow, based on the granular gases theory for the particle phase and the turbulent mixing length approach for the fluid phase. Hsu et al. (2004) present a two-phase sediment transport description, developed for strong turbulent shear flows over mobile beds.

Many recent works present a probabilistic approach to bedload transport, in which the motion of particles is modelled on the basis of probability density functions for velocities and grain accelerations, as well as grain path lengths and travel times (e.g. Furbish et al. 2012). However, Lagrangian modelling, although very precise and capable of determining exact paths of separate particles, is less effective when large datasets are considered. Therefore, DAM (Double-Averaging Methodology) methods are employed (e.g. Vowinckel et al. 2017a and 2017b).

The majority of models for wave-induced sediment transport calculate sediment transport at specified grain mobility conditions as averaged over the wave period. Although the quasi-steady approach may give reasonable predictions of the net sediment transport, many researchers (Van Rijn et al. 2007a, 2007b, 2007c, 2007d, Briganti et al. 2018) found, that unsteady behavior of the oscillatory flow significantly influences the sediment concentration and the resulting net transport. Both velocity and sediment concentration vary in time, being not necessarily in phase with each other. Hence, the prediction of sediment transport is a complex problem. The most advanced theoretical models (Hsu et al. 2004, Kaczmarek et al. 2004, Silva et al. 2006, Cheng et al. 2017), as well as experimental investigations (Ribberink & Al-Salem 1995, Cloin 1998, O'Donoghue & Wright 2004a, Dohmen-Janssen & Hanes 2002, Hassan & Ribberink 2003, van der A. et al. 2010, Schretlen 2012, Kaczmarek et al. 2015) describe the unsteady sediment transport by equations for wave-induced sediment velocities and concentrations.

The concept of vertical shear stress variation, recently introduced by Kaczmarek et al. (2019) for steady flow is extended here for a wave motion. The proposed description of vertical shear stress variation is also verified here by comparison of the numerical calculation results of the maximum shear stress at the bed during the wave period versus the results of direct stress measurements (Rankin & Hires 2000, Jiang & Baldock 2015). In order to explain the model modification a short discussion of the basic model equations and the calculation procedure are included in this paper. Further, like the previous numerical calculations for the wave motion, the present calculations are not limited to the resulting net sediment transport. Here, a multi-layer approach is used to calculate both progressive and reverse sediment transport streams with a full vertical structure of instantaneous concertation and velocity. The calculations were carried out for different grain size distributions. The calculation results were compared with the wave data including acceleration-skewed oscillatory flows and flows described by Stokes' first and second approximations.

2. Description of the multi-layer model

The multi-phase approach is used in present model. Considering a different physical processes that rule sediment transport at various distances above an immobile bed. The specification of layers up to water surface elevation is proposed as follows (Fig. 1): a dense layer with immobile Coulomb friction sublayer and upper dense mobile sublayer dominated by grain collisions. Further, a contact layer, in which particle collisions and turbulent lift cooperate in momentum exchange and suspended sediment zone.

Under conditions of high grain mobility the transport of concentrated sediment takes place at the entire layer of the dense mixture, in the form of a grain flow with a specific velocity and concentration profile. Under conditions of low grain mobility, the active layer is reduced to the upper sublayer, consisting of single grains being rolled and dragged over the bed surface, as in a typical bedload regime. Since it is assumed that both water and grains move in both regions (i.e. at the mobile dense layer and in the layer of suspended sediment), therefore, there must be a transitional zone between these two regions, in which both instantaneous velocity and concentration profiles of each fraction of the sediment mixture (Fig. 1a) and the shear stress profile (Fig. 1b) represent continuous shape. This transition zone is called the contact layer after Kaczmarek et al. (2004), Kaczmarek et al. (2017) and Kaczmarek et al. (2019).
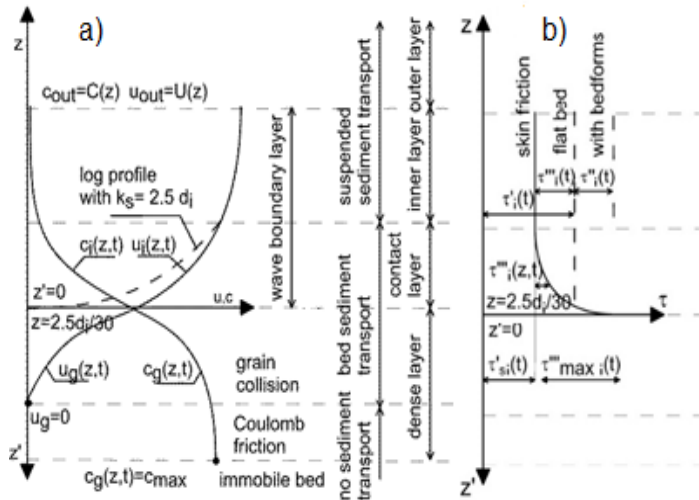

Fig. 1. Vertical structure of: a – instantaneous sediment transport (during the wave period) with velocity and concentration of the i-th fraction of sediment;
b – the instantaneous shear stress profile of the i-th fraction of sediments

The suspended sediment zone is divided into inner and outer flow regions. The inner flow region is characterized by a logarithmic velocity profile. The outer region of pure suspension is characterized by a very small concentration, where the process of sediment distribution may be considered as a convective or diffusive process. In contrast, the dense layer is characterized by very high concentrations, where inter-granular resistance is predominant.

The following mechanism of transmission of a tractive shear stress from the fluid to the immobile bed is proposed both for the wave motion and steady flow. The declining part of particle stresses in the upper dense sublayer is transferred directly to the moving grains. The increasing residual part as the rate-independent component is transferred further to the fixed bed. The concept of shear stress variation proposed originally for steady flow (Kaczmarek et al. 2019) is extended here for a wave motion. Shear stress increases from the skin stress value above the bed to the maximum value at the bed, and then, the viscous part of this stress decays in the bed. However, while the skin shear stress above the bed as an input data is identified with the value obtained from experiments at steady flow conditions, it must be calculated in the case of wave flow.

It is assumed (after Kaczmarek et al. 2004), that in the moving layer of densely concentrated sediments, all sediment fractions move at the velocity equal to the velocity of the mixture (at specified elevation). Therefore, it is assumed that interactions between the sediment fractions are so strong, that the finer fractions are slowed down by the thicker ones and all the fractions are characterised by the same vertical instantaneous velocity $u_g(z', t)$ and concentration $c_g(z', t)$ distributions. The model also takes into account, that the most intensive sorting of sediment occurs in the grain scattering process in the contact layer and in turbulent flow region, which brings the sediment into suspension. In the contact layer, instantaneous velocities $u_i(z, t)$ and concentrations $c_i(z, t)$ vary for individual fractions, due to turbulent fluid pulsations and chaotic collisions of grains.

The instantaneous grain stress components $\tau_i'''(z, t)$ of individual sediment fractions, which are all related to grain movement throughout the entire contact layer, change from zero at the upper boundary of the contact layer to the maximum value at the upper boundary of the dense layer (Fig. 1b). Hence, the maximum stresses during the wave period representative of the sediment mixture may vary from the stresses τ_r' at the upper boundary of the contact layer to τ_{0r} at the top of the dense layer. The maximum stresses τ_r' during the wave period at the upper boundary of the contact layer are the sum of skin shear stresses τ_{sr}' and stresses τ_r''', averaged over the depth, which result from grain movement across the entire contact layer. The skin shear stresses $\tau_{si}'(t) = \rho u_{fsi}'^2(t)$, where ρ is the density of water, and $u_{fsi}'(t)$ is the friction velocity, are

described here by the logarithmic profile with the skin hydraulic roughness, $k_{si} = 2{,}5d_i/30$. They are calculated by the Fredsøe (1984) model.

3. Basic equations and calculation procedure

Temporary profiles of the velocity $u_g(z', t)$ and concentration $c_g(z', t)$ in the dense layer are calculated using the equations Eq. (1) and Eq. (2) in a system of coordinates with the vertical axis z' directed downwards (Fig. 1a):

$$\alpha^0 \left(\frac{c_g - c_0}{c_m - c_g}\right) \sin \varphi \sin 2\psi + \mu_1 \left(\frac{\partial u_g}{\partial z'}\right)^2 = \tau_{0r} \tag{1}$$

$$\alpha^0 \left(\frac{c_g - c_0}{c_m - c_g}\right)(1 - \sin \varphi \cos 2\psi) + \mu_2 \left(\frac{\partial u_g}{\partial z'}\right)^2 = \left(\frac{\mu_2}{\mu_1}\right)\Big|_{c_g = c_0} \tau_{0r} + (\rho_s - \rho)\, g \int_0^{z'} c_g dz' \tag{2}$$

where $\tau_{0r}(t) = \rho u_{f0r}^2(t)$; u_{f0r} is the friction velocity at the top of the dense layer; $\alpha_0 = \text{constant} = \rho_s g d$; $d = d_r = d_{50}$ where d_r is the representative diameter for sediment mixture; $c_m = 0.53$ is the maximum concentration of the bed sediment; $c_0 = 0.32$ is the concentration of sediment at the upper limit of the dense layer; $\varphi = 24.4°$ is the quasi-static angle of internal friction; Ψ = angle between the major principal stress and the horizontal axis:

$$\psi = \frac{\pi}{4} - \frac{\varphi}{2} \tag{3}$$

μ_2, μ_1 = functions of concentration, described (after Sayed and Savage 1983) as

$$\mu_1 = \frac{0.03}{(c_m - c_g)^{1.5}} \rho_s d^2 \quad \text{and} \quad \mu_2 = \frac{0.02}{(c_m - c_g)^{1.75}} \rho_s d^2 \tag{4}$$

The stresses $\tau_{0r}(t)$ at the top of the dense layer are calculated by the integral model by Fredsøe (1984) using the results of a calculation procedure for maximum shear stress during the wave period describes by the Eq. (8-10).

The first component on the left-hand side of Eq. (1) describes the shear stress relation for plastic stresses, while the second component represents "viscous" stresses. Similarly, the first element on the left-hand side of Eq. (2) describes the normal stress relation for plastic stresses, while the second element describes normal "viscous" stresses. The combination of these stresses makes it possible to model both stresses related to the collision of grains, which disappear deeper into the dense mobile sublayer, and the residual part of stresses due to the tight inter-granular adhesion, which increases deeper into the dense immobile sublayer as a rate-independent component.

Assuming that settling of sediment balances the vertical exchange and the momentum exchange balances the shear stress, following Deigaard (1993) and Kaczmarek et al. (2004) a set of two differential equations is proposed to determine the instantaneous concentration and velocity profiles for the i-th sediment fraction in the contact layer:

$$\left[\frac{3}{2}\left(\alpha_s\frac{d}{w_s}\frac{\partial u_i}{\partial z}\frac{3}{2}\frac{s+c_M}{c_D}+\beta_i\right)^2 d_i^2 c_i^2(s+c_M)+l^2\right]\left(\frac{\partial u_c}{\partial z}\right)^2=u_{f*}'^2 \qquad (5)$$

$$\left[3\left(\alpha_s\frac{d_i}{w_{si}}\frac{\partial u_i}{\partial z}\frac{2}{3}\frac{s+c_M}{c_D}+\beta_i\right)^2 d_i^2\frac{\partial u_i}{\partial z}c_i+l^2\frac{\partial u_i}{\partial z}\right]\frac{\partial c_i}{\partial z}=-w_{si}c_i \qquad (6)$$

where w_{si} = settling velocity of the i-th fraction of sediment; c_M = added hydrodynamic mass coefficient; c_D = 1.0 is a drag coefficient; l = mixing length equal to κz; κ = von Karman's constant, which is around 0.40; s = ρ_s/ρ is the relative density; ρ_s is the density of sediments; (s+c_m) = 3.0. Coefficients $\alpha_i = \beta_i$ are calculated by an iteration procedure, assuming the equality of the calculated sediment velocity $u_i(z,t)$ and the logarithmic flow velocity at the upper limit of the boundary layer at the time of the maximum skin shear stresses during the wave period.

To calculate the instantaneous sediment transport intensity, the instantaneous concentration and velocity profiles of the i-th fraction of the sediment are calculated in individual layers using the system of equations Eq. (1) and Eq. (2) for the dense layer and the system of equations Eq. (5) and Eq. (6) for the contact layer. Then, the instantaneous sediment transport rate for the i-th sediment fraction is calculated by integrating the instantaneous vertical streams throughout the entire flow region:

$$q_i(t)=\int_0^{\delta_g}\left|u_g(z',t)\right|c_g(z',t)dz'+\int_{\frac{k_{si}}{30}}^{\frac{k_{si}}{30}+\delta_c}|u_i(z,t)|c_i(z,t)dz+\int_{\frac{k_{si}}{30}+\delta_c}^{\frac{k_{si}}{30}+\delta_{\frac{1}{2}}'}|u_i(z,t)|c_i(z,t)dz=$$

$$\int_0^{\delta_g}\left|u_g(z',t)\right|c_g(z',t)\mathrm{d}z'+\int_{\frac{k_{si}}{30}}^{\frac{k_{si}}{30}+\delta_{\frac{1}{2}}'}|u_i(z,t)|c_i(z,t)\mathrm{d}z \qquad (7)$$

where $\delta_{1/2}'$, is the thickness of the wave boundary layer, δ_c and δ_{in} are the thicknesses of the contact layer and the inner layer, respectively.

The instantaneous sediment transport is calculated only for the wave boundary layer. This is because it can be expected outside this layer (according to Kaczmarek et al. 2004), that transport of sediment depends only on the average velocity during the wave period (Fig. 1a), which is equal to zero in pure wave motion. The knowledge of the instantaneous sediment transport intensity for the *i*-th sediment fraction allows to calculate sediment transport for all sediment fractions.

It is worth noting that all sediment fractions in the dense layer move at a velocity equal to the velocity of the mixture. This assumption allows to take into account the hiding and exposure effects which can affect the transport rates of sediment grain fractions in the dense layer. Coarser sediments in the mixture are more exposed to the flow, whereas thinner sediments are hiding among the coarser ones.

Following the idea by Kaczmarek et al. (2019), the three mobile-bed effect parameters are introduced:

$$\gamma_0 = \sqrt{\frac{\tau_{0r}}{\tau'_{sr}}} = \frac{u_{f0r}}{u'_{fsr}} \tag{8}$$

In order to find the parameters γ_0 it is assumed that sediment transport in the dense and contact layers, calculated for maximum relative shear stresses during the wave period, can be compared to values calculated by the Meyer-Peter and Müller (1948) semi-empirical formula (MPM).

Then, the following equation is postulated (Kaczmarek et al. 2019):

$$q_g\left(\rho\gamma^2 u'^2_{fsr}\right) + q_c\left(\rho u'^2_{fsr}\right) = \Phi_{MPM}\sqrt{(s-1)g d_r^3} \tag{9}$$

The parameter $\gamma = \gamma_0$ in Eq. (9) is sought by the iterative method. The value q_g denotes sediment transport in the grain collision sublayer caused by the shear stresses τ_{0r}, whereas q_c denotes sediment transport in the contact layer caused by the shear stress τ'_r. The right-hand side of Eq. (9) expresses sediment transport described by the MPM formula:

$$\Phi_{MPM} = 8(\theta_r' - \theta_c)^{1.5} \text{ where } \theta_r' = \frac{u'^2_{fr}}{g(s-1)d} \tag{10}$$

The non-dimensional critical stresses θ_c are assumed to be constant over the contact layer thickness (Fig. 1b) and equal to 0.05.

4. Calculation results against measurements

The calculations of γ_0 (Fig. 2) were carried out for King's (1991) experiments, for both sine waves and asymmetrical waves, characteristic for waves described by Stokes' second approximation and for acceleration-skewed waves. King's (1991) experiments were performed for three grain diameters: d = 0.135 mm, 0.44 mm and 1.1 mm.

Comparison of the calculated γ_0 with the results of experiments by Rankin and Hires (2000) for d = 0.23 mm and by Jiang and Baldock (2015) for d = 0.22 mm and 2.83 mm shows that there are no major differences between the calculated and measured values, although there are clear differences between results for Stokes' approximations and results for skewed waves. The calculated values of γ_0 for skewed waves are smaller than those for the waves described by Stokes' first approximation (sine wave) and Stokes' second approximation (asymmetrical wave). This difference (of up to 0.75 γ_0 for d = 1.1 mm, 0.8 γ_0 for d = 0.44 mm and 0.65 γ_0 for d = 0.135 mm) occurs regardless of the grain diameter, although the calculated values of γ_0 are not smaller than the values measured by Jiang and Baldock (2015) for the diameter d = 2.83 mm (Fig. 2).
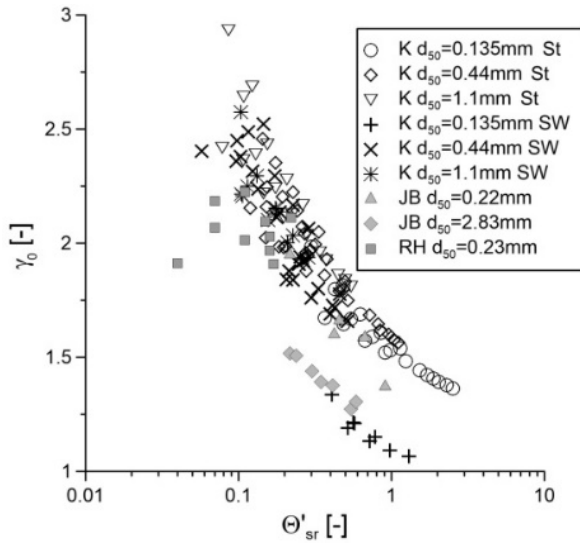
Fig. 2. Comparison of calculated γ_0 for sine waves and asymmetrical waves described by Stokes' approximations (St) and skewed waves (SW) from the experiment by King (1991) (K) with measurement data for γ_0 by Jiang and Baldock (2015) (JB) and Rankin and Hires (2000) (RH)

Fig. 3a compares calculated and measured values of the total sediment transport q_t. The data used for comparison come from measurements in full-scale oscillating tunnels with well-sorted semi-uniform sediments. Those measurements were carried out both for asymmetrical waves described by Stokes' second approximation (Ribberink & Al-Salem 1995, Hassan & Ribberink 2003) and for acceleration-skewed waves (van der A. et al. 2010).

The experimental data used for comparison (Fig. 3b) also come from full-scale oscillating tunnels (Cloin 1998, Hassan & Ribberink 2003), but with poorly sorted sediments. It can be seen that the present model reproduces the measured values of the total sediment transport q_t and q_{ti} within plus/minus a factor of two of measurements, regardless of the wave shape. The model also maps the values of the measured total transport q_t due to acceleration-skewed waves almost perfectly (Fig. 3a) when the bed is built of well-sorted, almost homogeneous sediment. It is worth noting that even great discrepancies in net sediment transport do not result in significant differences between calculated and measured values of total sediment transport q_t and q_{ti}. Agreement within plus/minus a factor of two of measurements is achieved.
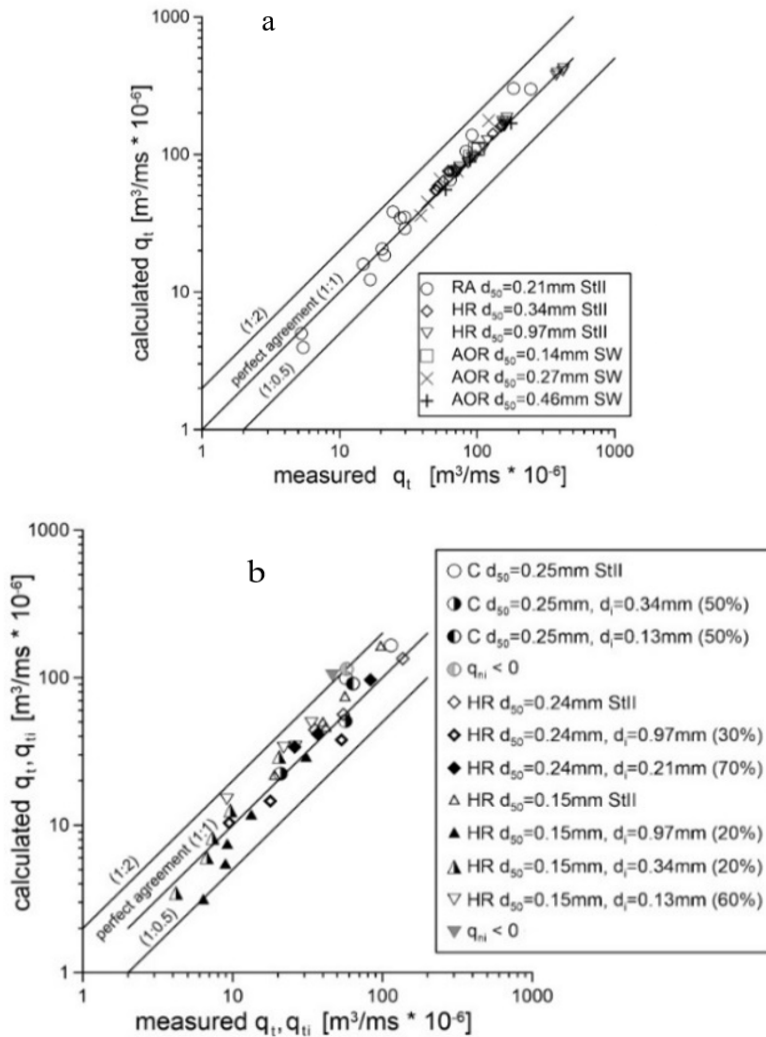
Fig. 3. Comparison of calculated and measured values of: a – total sediment transport q_t for well-sorted semi-uniform sediments; b – total sediment transport q_t and q_{ti} for poorly sorted sediments; RA: Ribberink and Al-Salem (1995), HR: Hassan and Ribberink (2003), AOR: van der A. et al. 2010), C: Cloin (1998), StII – Stokes second approximation, SW – Skewed waves

Fig. 4, also compares calculated and measured values of q_t. Here, the experimental data come from small-scale flumes (Kaczmarek 2004, Kaczmarek et al. 2015) and full-scale flumes (Schretlen 2012, Dohmen-Janssen & Hanes 2002), where both the effect due to the presence of bed forms (Kaczmarek 2004, Kaczmarek et al. 2015) and the streaming effect (Schretlen 2012, Dohmen-Janssen & Hanes 2002) on sediment transport are expected.
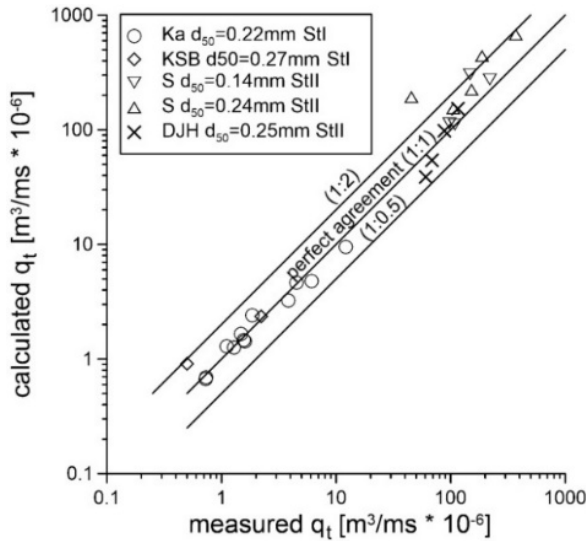

Fig. 4. Comparison of calculated and measured values of the total sediment transport q_t (Ka: Kaczmarek 2004, KSB: Kaczmarek et al. 2017, S: Schretlen 2012, DJH: Dohmen-Janssen & Hanes 2002). StI: Stokes' first approximation, StII: Stokes' second approximation

These effects can influence the modelled sediment transport mainly in the inner layer. They are not considered in the present model. This is the cause of the discrepancy between the experimental and modelled results. However, for the calculated total sediment transport, agreement within plus/minus a factor of two of measurements is achieved. The consistency of the results does not depend on the scale of experiments (full-scale or small-scale). The measurements analysed include those for symmetrical waves described by Stokes' first approximation (Kaczmarek 2004, Kaczmarek et al. 2015) and those for asymmetrical waves described by Stokes' second approximation (Schretlen 2012, Dohmen-Janssen & Hanes 2002).

5. Conclusions

The comparison of numerical calculations of total sediment transport with measurements indicates that the multi-layer model reproduces measured values within plus/minus a factor of two, regardless of the wave shape. The calculations were carried out for any grain size distribution of bed sediments, including well-sorted semi uniform and poorly sorted grains. Even great discrepancies in net sediment transport values for fine sediments do not result in significant differences between the calculated and measured values of total sediment transport. Then, the consistency of total sediment transport within plus/minus a factor of two of measurements is still achieved. The model also maps the values of the measured total transport almost perfectly when the bed is built of well-sorted, almost homogeneous sediment.

The comparison of numerical calculations with measurements shows that the multi-layer model can be applied to a very wide range of grain mobility conditions, including both non-intensive sediment transport and fully developed, intensive sediment transport under sheet flow conditions. To obtain a solution, only few measurable parameters are needed as input, and no additional calibration is needed. The above features make the model of potential engineering interest.

References

Berzi, D., & L. Fraccarollo. (2016). Intense sediment transport: Collisional to turbulent suspension. *Phys. Fluids, 28*(2): 023302. DOI: 10.1063/1.4941770.

Briganti, R., N. Dodd, G. Incelli, & G. Kikkert. (2018). Numerical modelling of the flow and bed evolution of a single bore-driven swash event on a coarse sand beach. *Coastal Eng., 142*, 62-76. DOI: 10.1016/j.coastaleng.2018.09.006.

Cheng, Z., T.-J. Hsu, & J. Calantoni. (2017). SedFoam: A multi-dimensional Eulerian two-phase model for sediment transport and its application to momentary bed failure. *Coastal Eng., 119,* 32-50. DOI: 10.1016/j.coastaleng.2016.08.007.

Cloin, B. (1998). Gradation effects on sediment transport in oscillatory sheet-flow. *Prog. Rep. H2305.* Delft, Netherlands: WL/Delft Hydraulics.

Deigaard, R. (1993). Modelling of sheet flow: Dispersion stresses versus the diffusion concept. *Prog. Rep. Lyngby, Denmark: ISVA.* Technical Univ. of Denmark.

Dohmen-Janssen, C. M., & D. M. Hanes. (2002). Sheet flow dynamics under monochromatic nonbreaking waves. *J. Geophys. Res., 107*(C10), 3149. DOI: 10.1029/2001JC001045.

Fredsøe, J. (1984). Turbulent boundary layer in combined wave-current motion. *J. Hydraul. Eng. 110*(8), 1103-1120.

Furbish, D. J., P. K. Haff, J. C. Roseberry, & M.W. Schmeeckle. (2012). A probabilistic description of the bed load sediment flux: 1. Theory. *J. Geo-Phys. Res. Earth Surf. 117*(F3): 3031. DOI: 10.1029/2012JF002352.

Hassan, W.N., & J.S. Ribberink. (2003). Transport processes of uniform and mixed sands in oscillatory sheet flow. *Coastal Eng. 52*, 745-770. DOI: 10.1016/j.coastaleng.2005.06.002.

Hsu, T., & J. T. Jenkins. (2004). On two-phase sediment transport: Sheet flow of massive particles. *Proc. R. Soc. Lond.* A 460 (2048), 2223-2250. DOI: 10.1098/rspa.2003.1273.

Jiang, Z., & T. E. Baldock. (2015). Direct bed shear measurements under loose bed swash flows. *Coastal Eng.,* 100, 67-76. DOI: 10.1016/j.coastaleng.2015.04.0010378-3839.

Kaczmarek, L. M., J. Biegowski, & R. Ostrowski. (2004). Modelling cross-shore intensive sand transport and changes of bed grain size distribution versus field data. *Coastal Eng., 51*(5-6), 501-529. DOI: 10.1016/j.coastaleng.2004.05.007.

Kaczmarek, L. M., S. Sawczyński, & J. Biegowski. (2015). Hydrodynamic equilibrium for sediment transport and bed response to wave motion. *Acta Geophys., 63*(2), 486-513. DOI: 10.1515/acgeo-2015-0008.

Kaczmarek, L. M., S. Sawczyński, & J. Biegowski. (2017) An equilibrium transport formula for modeling sedimentation of dredged channels. *Coastal Eng. J., 59*(3), 1750015-1750015-35. DOI: 10.1142/S0578563417500152.

Kaczmarek, L. M., J. Biegowski, & Ł. Sobczak. (2019). Modeling of Sediment Transport in Steady Flow over Mobile Granular Bed. *J. Hydraul. Eng., 145*(4), 04019009. DOI: 10.1061/(ASCE)HY.1943-7900.0001566.

King, D.B. (1991). *Studies in oscillatory flow bedload sediment transport.* PhD Thesis. USA, San Diego: Univ. of California.

Meyer-Peter, E., & R. Müller. (1948). Formulas for bed-load transport. In Proc., 2nd Meeting of the Int. Association for Hydraulic Structures Research. Delft, Netherlands: *International Association for Hydro-Environment Engineering and Research.*

O'Donoghue, T., & S. Wright. (2004a). Concentrations in oscillatory sheet flow for well sorted and graded sands. *Coastal Eng., 50*(3), 117-138. DOI: 10.1016/j.coastaleng.2003.09.004.

Rankin, K. L., & R. I. Hires. (2000). Laboratory measurement of bottom shear stress on a movable bed. *J. Geo-Phys. Res. – Oceans., 105*(C7) 17011-17019. DOI: 10.1029/2000JC900059.

Ribberink, J. S., & A. Al-Salem. (1995). Sheet flow and suspension of sand in oscillatory boundary layers. *Coastal Eng., 25*(3-4), 205-225. DOI: 10.1016/0378-3839(95)00003-T.

Schretlen, J.L.M. (2012). *Sand transport under full-scale progressive surface waves.* PhD thesis. Enschede, Netherlands: Univeristy of Twente.

Silva, P. A., A. Temperville, & F. S. Santos. (2006). Sand transport under combined current and wave conditions: A semi-unsteady, practical model. *Coastal Eng., 53*(11), 897-913. DOI: 10.1016/j.coastaleng.2006.06.010.

Van der A, D. A., T. O'Donoghue, & J. S. Ribberink. (2010). Measurements of sheet flow transport in acceleration-skewed oscillatory flow and comparison with practical formulations. *Coastal Eng., 57*(3), 331-342. DOI: 10.1016/j.coastaleng.2009.11.006.

Van Rijn, L. C. (2007a). Unified view of sediment transport by currents and waves. I: Initiation of motion, bed roughness and bed-load transport. *J. Hydraul. Eng.*, *133*(6), 649-667.

Van Rijn, L. C. (2007b). Unified view of sediment transport by currents and waves. II: Suspended transport. *J. Hydraul. Eng.*, *ASCE, 133*(6), 668-689.

Van Rijn, L. C. (2007c). Unified view of sediment transport by currents and waves. III: Graded beds. *J. Hydraul. Eng., ASCE, 133*(7), 761-775.

Van Rijn, L. C., D.J.R. Walstra, & M van Ormondt. (2007d). Unified view of sediment transport by currents and waves. IV: Application of morphodynamic model. *J. Hydraul. Eng.*, *ASCE, 133(7)*, 776-793.

Vowinckel, B., V. Nikora, T. Kempe, & J. Fröhlich. (2017a). Momentum balance in flows over mobile granular beds: Application of double averaging methodology to DNS data. *J. Hydraul. Res., 55*(2), 1-18. DOI: 10.1080/00221686.2016.1260656.

Vowinckel, B., V. Nikora, T. Kempe, & J. Fröhlich. (2017b). Spatially averaged momentum fluxes and stresses in flows over mobile granular beds: A DNS-based study. *J. Hydraul. Res. 55*(2), 208-223. DOI: 10.1080/00221686.2016.1260658.